Regional Pulmonary Perfusion Following Human Heart-Lung Transplantation

Robert Lisbona, Tawfic S. Hakim, Geoffrey W. Dean, David Langleben, Albert Guerraty, and Robert D. Levy

Department of Nuclear Medicine, Division of Cardiovascular Surgery, and Division of Respiratory Medicine, Royal Victoria Hospital; Division of Cardiology, Sir Mortimer B. Davis Jewish General Hospital; and Department of Physiology, McGill University, Canada

Ventilation and perfusion scans were obtained in six subjects who had undergone heart-lung transplantation with consequent denervation of the cardiopulmonary axis. Two of the subjects had developed obliterative bronchiolitis, which is believed to be a form of chronic rejection. Their pulmonary function tests demonstrated airflow obstruction and their scintigraphic studies were abnormal. In the remaining four subjects without obstructive airways disease, ventilation and planar perfusion scans were normal. Single photon emission computed tomography imaging of pulmonary perfusion in these patients revealed a layered distribution of blood flow indistinguishable from that of normal individuals. It is concluded that neurogenic mechanisms have little influence on the pattern of local pulmonary blood flow at rest.

J Nucl Med 30:1297–1301, 1989

Heart-lung transplantation for end-stage cardiopulmonary disease is presently an accepted therapeutic approach in selected individuals (*1–3*). The procedure will allow patients with debilitating chronic disease to lead comfortable and productive lives. The nature of ventilation in the post-transplant lungs has been documented by pulmonary function testing in clinically well transplanted subjects (*4–7*). Little information, however, is available concerning the pattern of regional pulmonary perfusion in these patients who have undergone denervation of the cardiopulmonary axis at the time of transplantation.

MATERIALS AND METHODS

The subject population consisted of six subjects who underwent heart-lung transplantation for end stage cardiopulmonary disease. Patient characteristics are seen in Table 1. They were all females who ranged in age from 24 to 40 yr. The average period after transplantation at the time of assessment was 10.5 mo (range 2–31 mo). The patients were clinically well and had normal chest radiographs at the time of study. They had no recent acute rejection episode and had normal cardiac function at investigation, which included radionuclide gated cardiac studies, endomyocardial biopsy and clinical evaluation. All subjects underwent pulmonary function tests (PFTs) within 2 wk of the nuclear studies with measurements of forced expiratory flow rates, lung volumes (body plethysmography), single breath diffusion of carbon monoxide (D_LCO) and arterial blood gases.

Ventilation and perfusion studies of the lungs were obtained in the department of nuclear medicine. The ventilation scans consisted of right and left posterior oblique images after the inhalation of a bolus of 10 mCi of xenon-133 (^{133}Xe). The study included a wash-in, equilibrium, and wash-out phase generated over 5 min in a closed system. Subsequently, the patients were injected intravenously in the supine position with 5 mCi of technetium-99m macroaggregated albumin ([^{99m}Tc]MAA). Perfusion scans were then done and planar images of 1 million counts each were registered in the six standard positions with a large field-of-view camera equipped with a low-energy general purpose collimator. A single photon emission computerized tomographic (SPECT) study of pulmonary perfusion was also undertaken after positioning the thorax within the field of view of an integrated tomographic system (Omega 500-MCS 560, Technicare, Solon, OH) with a low-energy high resolution collimator. One-hundred twenty projections of the lungs were registered from a circular orbit in 128 × 128 matrices and in 3-degree steps around the subjects who were instructed to breathe normally. Each projection was generated over 15 sec and accumulated 100,000 counts. The data were then reconstructed by filtered backprojection using a third order Butterworth filter with a cutoff frequency of 0.3 times the Nyquist frequency of 0.125 cm^{-1}. Tomographic sections 11 mm thick were generated in the transverse, sagittal, and coronal planes. There was no attenuation correction. Pixels with a value of <10% of the maximal

Received Nov. 18, 1988; revision accepted Mar. 29, 1988.

For reprints contact: Robert Lisbona, MD, Nuclear Medicine Department, Royal Victoria Hospital, 687 Pine Ave. West, Montreal, Quebec, Canada H3A 1A1.

TABLE 1
Patient Profiles

Patient	Age/sex	Diagnosis	Time from transplant to scans	Ventilation scan	Perfusion scan	LVEF*
1	39/F	Emphysema	9 mo	N	N	63%
2	35/F	VSD Eisenmenger reaction	8 mo	N	N	57%
3	24/F	Lupus erythematosus	4 mo	N	N	71%
4	40/F	Alpha-1 antitrypsin deficiency	2 mo	N	N	70%
5	38/F	Primary pulmonary arterial hypertension	9 mo	Retention at level of upper lobes	Nonhomogeneous perfusion	82%
6	31/F	Alpha-1 antitrypsin deficiency	31 mo	Retention at level of upper lobes	Small peripheral perfusion defects in upper lobes	74%

* Left ventricle ejection fraction by radionuclide gated cardiac angiography.
Normal = 62% ± 10 ejection fraction units.

activity of a slice were set to zero in order to remove remaining reconstruction artifacts from each slice. This process also defined the edge of the lung on the image since our previous experiments have revealed that, at that threshold value, the one to one image of a tomographic slice corresponds most closely in actual size to the dissected equivalent slice from the animal lung (*8–11*). Thereafter, mappings of the distribution of radioactivity were created from the sections. The data were then compared to normal standards established in our laboratory (*8–11*). The average distribution of perfusion was also calculated for each individual coronal slice so as to obtain a graph of the mean distribution of blood flow in the vertical axis along the gravity vector. This was done by summing the activity in each slice and normalizing it to the number of pixels in that slice.

RESULTS

Results of PFTs are seen in Table 2. Subjects 1 and 2 had studies suggestive of very mild restrictive abnormalities with increased FEV_1/FVC ratios, but normal lung volumes. Subjects 3 and 4 had mild to moderate restrictive abnormalities with a reduced TLC (76% predicted) noted in subject 3. Airways resistance and D_LCO were normal in subjects 1–4. Subjects 5 and 6 had PFTs indicative of mild and severe small airways airflow obstruction, respectively. Both of these patients had clinical courses compatible with the development of bronchiolitis obliterans. All subjects had PaO_2 values of greater than 75 mmHg on room air.

The first four subjects had normal ventilation studies on ^{133}Xe imaging. As well, the planar images of perfusion were within normal limits in these individuals. The two subjects with obliterative bronchiolitis had abnormal ventilation studies with evidence of trapping of radioactive xenon at the level of the upper lobes. One of those patients (subject 5), with only mild obliterative bronchiolitis, had nonhomogeneous perfusion of the lungs without distinct defects. The other patient (subject 6), had severe bronchiolitis which manifested on the perfusion scan as multiple small focal abnormalities of flow primarily in the regions of abnormal ventilation.

The analysis of the SPECT data in subjects 1–4 revealed that the pattern of regional pulmonary perfusion at rest was normal. The tomographic studies are presented in two forms: (a) the distribution of flow

TABLE 2
Pulmonary Function

Patient no.	FEV1* L	FVC* L	FEV1/FVC %	RV* L	TLC* L	D_LCO* ml/min/mmHg	Raw† $cmH_2O/L/S$	PImax‡ cmH_2O
1	2.86 (107)	2.95 (86)	97	1.80 (114)	4.42 (88)	25.7 (110)	1.43	−58 (−76 ± 25)
2	2.69 (109)	3.00 (96)	90	1.21 (100)	4.16 (96)	22.0 (98)	1.16	−68 (−76 ± 25)
3	2.90 (90)	3.05 (76)	95	1.15 (74)	4.20 (76)	29.9 (116)	0.73	−130 (−89 ± 17)
4	1.94 (70)	2.12 (59)	92	2.16 (108)	4.52 (86)	27.5 (105)	2.39	−110 (−76 ± 25)
5	1.78 (68)	2.57 (77)	69	1.96 (133)	4.51 (94)	18.4 (79)	2.89	−140 (−76 ± 25)
6	0.98 (36)	1.83 (53)	53	2.27 (171)	4.46 (93)	14.6 (62)	3.67	−73 (−76 ± 25)

FEV1 = forced expiratory volume in 1 sec; FVC = forced vital capacity; RV = residual volume; TLC = total lung capacity; D_LCO = single breath diffusing capacity for carbon monoxide; Raw = airway resistance; PImax = maximum occluded inspiratory mouth pressure.
* Values in brackets are % of predicted values calculated for the recipient.
† Normal 95% confidence limits 0.2–2.5.
‡ Values in brackets are mean ± s.d.

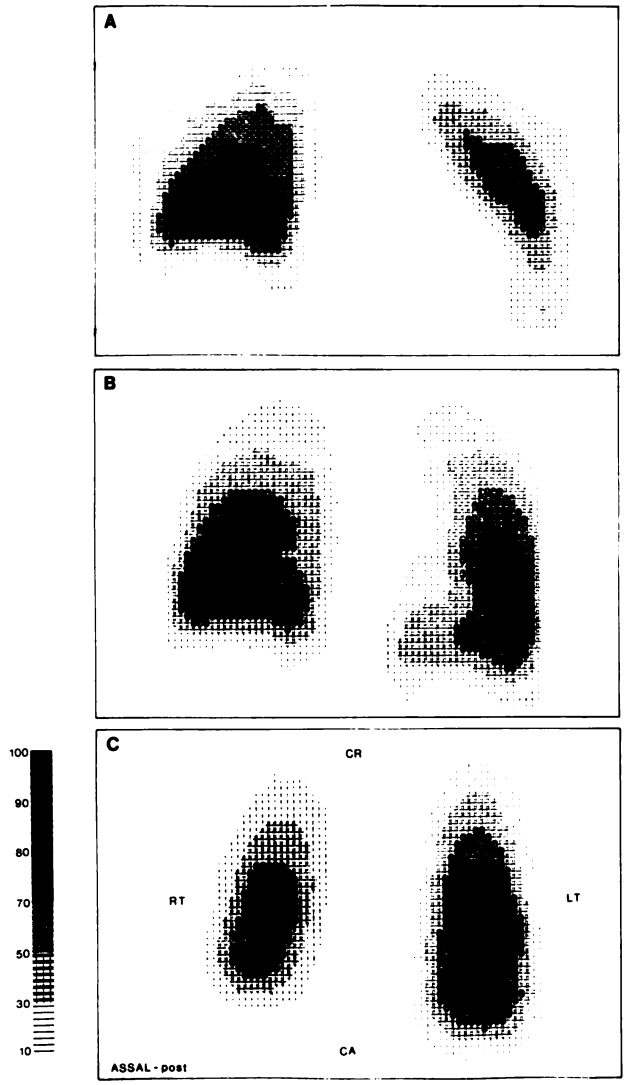

FIGURE 1
Mapping of blood flow distribution in three coronal slices from subject 1 9 mo post heart-lung transplant. The slices are from a mid-lung plane (B middle panel), a ventral plane (A top panel) and from a dorsal plane (C bottom panel). Because the subject was injected supine, regional differences within each slice are independent of gravity. The image of each slice was mapped using the scale shown. Activity (or blood flow) per voxel was expressed as % of maximum value within the slice. Values <10% were excluded. Note the concentric pattern in flow distribution in all three slices. The orientation is indicated in one panel: CA = caudal; CR = cranial; LT = left; RT = right.

within a given slice to demonstrate the interregional differences in flow distribution as reported by our laboratory (*8–11*), and (b) the average vertical distribution of flow to describe the vertical zonal differences as described by West et al. (*12,13*). Examples of tomographic mappings of regional blood flow in coronal slices from subject 1 with normal ventilation and planar perfusion scans are shown in Figure 1. The mappings revealed a pattern of regional blood flow distribution similar to that of normal subjects. The blood flow was distributed nonuniformly with marked regional differences characterized by preferential perfusion to the center of the slice with a gradual decrease toward the periphery to reach a minimal value at the pleural edge. This pattern of perfusion was present at every tomographic coronal level. Since a coronal plane is influenced uniformly by the force of gravity, the pattern of concentric rings is independent of gravity. The central to peripheral ratio of perfusion was as high as 10:1 based on our definition of the edge of the lung. Figure 2 shows the mapping of flow distribution in a sagittal slice from the middle of the right lung in subject 1. This image revealed that, as in normal subjects, flow was distributed nonuniformly in a concentric pattern. In all sagittal slices, the pattern was also concentric with the central peak region closer to the dorsal edge of the slice, suggesting that besides the horizontal inequalities, flow is also influenced by the force of gravity. The average flow per unit lung volume in each coronal slice is illustrated in Figure 3 for the same subject. In general, flow was lowest in the ventral slices, increased gradually reaching maximum in the lower one third of the lung, and decreased again in the most dorsal slices. This pattern is typical of normal subjects and reflects the vertical zonal distribution of blood flow in the lung according to zones 1,2,3, and 4 of West et al. (*12,13*).

DISCUSSION

Combined heart-lung transplantation (HLT) is a procedure essentially reserved for selected patients with end-stage irreversible cardiopulmonary disease. The operation itself consists of en bloc HLT with anastomosis of the trachea, aorta, and a cuff of right atrium from the donor. It also results in cardiac and pulmonary denervation due to the inevitable resection of sympathetic and parasympathetic cardiopulmonary fibers of both donor and recipient. The phrenic nerves to the recipient's diaphragm are preserved, however, in order to maintain diaphragmatic function and chest wall mechanics. The extent of reinnervation of the transplanted lungs in humans is not known, but it would be reasonable to suggest that several months post-HLT, the lungs are functionally denervated (*14*). Thus, the HLT patients represent an ideal population for the evaluation of the effect of neurogenic mechanisms on regional pulmonary blood flow. Nevertheless, normal ventilation must first be documented in these patients since the study of the pulmonary circulation cannot be dissociated from that of ventilation.

Ventilation is one of the prime determinants of regional perfusion with abnormal aeration causing vasoconstriction and redistribution of local blood flow away from poorly ventilated regions. There may be ventilatory disturbances post-HLT which can be of a restrictive or an obstructive nature. Obliterative bronchiolitis, which is probably a form of chronic rejection of the

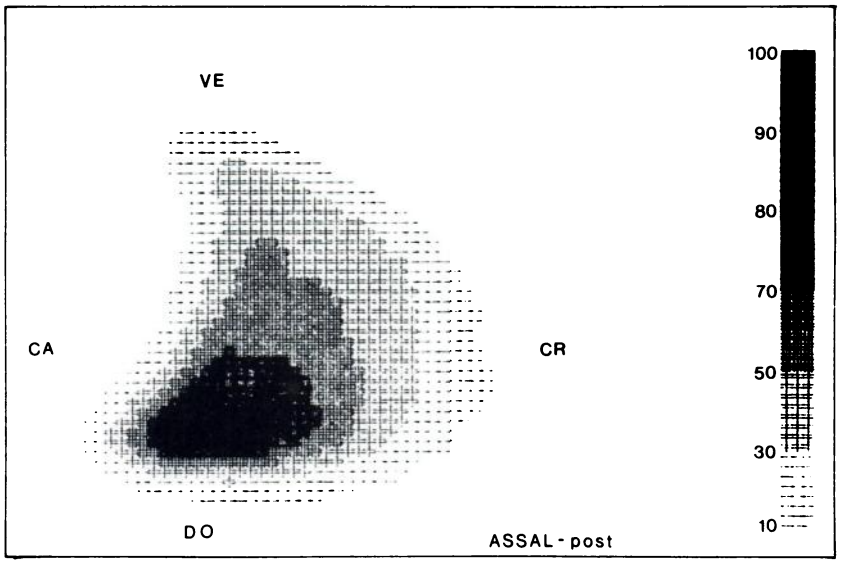

FIGURE 2
Mapping of blood flow distribution in a sagittal slice from the middle of the right lung of the same subject as in Figure 1. The concentric pattern of flow distribution is again noted. The zone of maximal flow is close to the most dependent edge of the lung indicating the effect of gravity in the vertical plane. The scale is the same as in Figure 1. Orientation of the slice is indicated: CA = caudal; CR = cranial; VE = ventral; DO = dorsal.

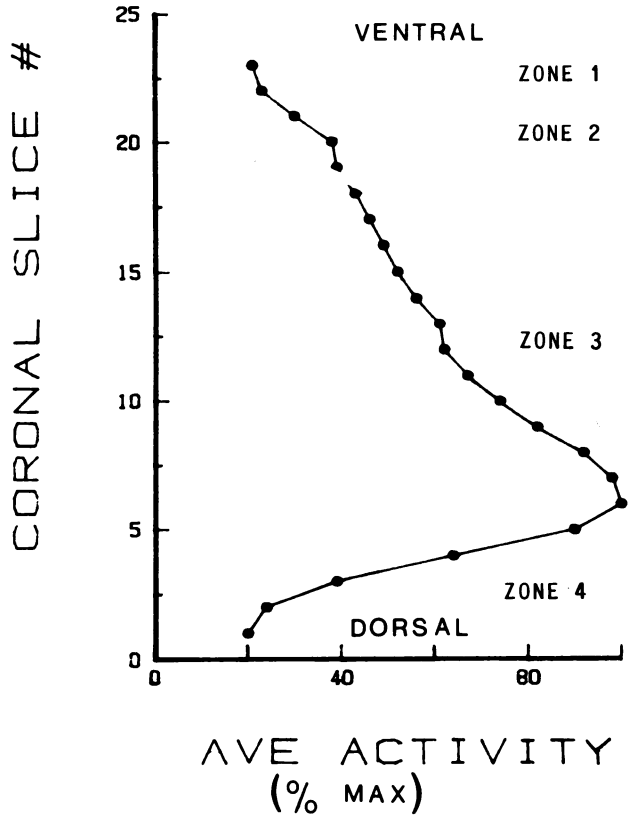

FIGURE 3
Profile of the average activity in the horizontal planes (subject 1). The average activity was calculated by dividing the total activity in each plane, by the total number of voxels. The activity is expressed as % of the maximum average. The pattern reflects the normal and gradual increase in average blood flow through West's Zone 1-3 band the subsequent fall in zone 4 (Ref. *12*).

pulmonary allograft (*6,15*), can induce an obstructive abnormality. Two of our patients developed this complication. Also, previous investigators have demonstrated that a stable restrictive ventilatory impairment is often seen post-HLT (*4,7*). This impairment is thought to be a result of both volumetric constraints of the recipient chest cavity and impaired contractility and/or efficiency of the respiratory muscles, rather than an intrinsic abnormality of the pulmonary parenchyma and its elastic properties (*7*). As such, abnormalities of the chest wall and/or respiratory muscles would not be expected to alter regional ventilation of the lungs except in extreme cases of the former, such as scoliosis (*16*). Hence, in our four remaining subjects, this mild restrictive limitation was not believed to affect regional ventilation and secondarily local perfusion. In these subjects, therefore, a stable ventilatory status confirmed by PFTs and radioxenon imaging favored a normal pattern to the distribution of regional blood flow allowing for the isolated study of the impact of pulmonary denervation on regional perfusion.

The lung tissues normally are innervated by autonomic fibers from the parasympathetic and sympathetic nervous systems. Their effect on the normal control of pulmonary blood flow is believed to be of minor consequence (*17*). In general, stimulation of the vagal fibers to the lungs slightly decreases pulmonary vascular resistance, while stimulation of the sympathetics causes a modest increase in vascular resistance. The normal pattern of regional blood flow demonstrated in the heart-lung transplant subjects studies indicates that indeed innervation is of marginal importance in the control of the local distribution of pulmonary blood flow at rest. Whether this three-dimensional pattern changes in patients during exercise is not clear at the present

time. The role of circulating catecholamines in these patients both at rest and during exercise is also still unknown.

Our previous experiments have indicated that gravity, although a factor, does not play a unique role in determining pulmonary perfusion at the regional level, since stratification of flow exists in lung zones which are subject to an equal force of gravity (*8–11*). Our current observations now stress the minimal effect of denervation on regional perfusion. It seems quite likely therefore that the inherent layered pattern of pulmonary blood flow reflects the varying resistance of the vascular circuitry. Conceivably, in the lung periphery, there is increased resistance to local flow induced by the long and branching delivery pathways of the vessels which, emanating from the central main arteries, perfuse the distant lung. This resistance can moderate the magnitude of outward flow and help confine perfusion to the shorter and lower resistance channels in the inner lung. The geometry of the pulmonary vascular tree may thus, to a large extent, dictate the distribution of regional flow.

In conclusion, the results of this study indicate that regional pulmonary perfusion is normal at rest in patients with denervation of the cardiopulmonary axis following heart-lung transplantation. This suggests that neurogenic mechanisms probably have little impact on resting blood flow distribution in the normal lung.

ACKNOWLEDGMENT

Dr. Langleben is a Research Scholar of the Canadian Heart Foundation.

REFERENCES

1. Reitz BA, Wallwork MB, Hunt SA, et al. Heart-lung transplantation. Successful therapy for patients with pulmonary vascular disease. *N Engl J Med* 1982; 306:557–564.
2. Griffith BP, Hardesty RL, Trenton A, et al. Heart-lung transplantation: lessons learned and future hopes. *Ann Thor Surg* 1987; 43:6–16.
3. Starnes VA, Jamieson SW. Current status of heart and lung transplantation. *World J Surg* 1986; 10:442–9.
4. Theodore J, Jamieson SW, Burke CM, et al. Physiologic aspects of human heart-lung transplantation. *Chest* 1984; 86:3, 349–357.
5. Theodore J, Morris AJ, Burke CM, et al. Cardiopulmonary function at maximum tolerable constant work rate exercise following human heart-lung transplantation. *Chest* 1987; 93:3, 433–439.
6. Glanville AR, Baldwin JC, Burke CM, Theodore J, Robin ED. Obliterative bronchiolitis after heart-lung transplantation: apparent arrest by augmented immunosuppression. *Ann Intern Med* 1987; 107:300–304.
7. Glanville AR, Theodore J, Harvey J, Robin ED. Elastic behavior of the transplanted lung. *Am Rev Respir Dis* 1988; 137:308–312.
8. Lisbona R, Dean GW, Hakim TS. Observations with SPECT on the normal regional distribution of pulmonary blood flow in gravity independent planes. *J Nucl Med* 1987; 28:1758–1762.
9. Hakim TS, Lisbona R, Dean GW. Gravity-independent inequality in pulmonary blood flow in humans. *J Appl Physiol* 1987; 63:3, 1114–1121.
10. Hakim TS, Dean GW, Lisbona R. Quantification of spatial blood flow distribution in isolated canine lung. *Invest Radiol* 1988; 23:7, 498–504.
11. Hakim TS, Dean GW, Lisbona R. Effect of body posture on spatial distribution of pulmonary blood flow. *J Appl Physiol* 1988; 64:3, 1160–1170.
12. West JB, Dollery CT, Naimark A. Distribution of blood flow in isolated lungs. Relation to vascular and alveolar pressures. *J Appl Physiol* 1964; 19:713–724.
13. Hughes JMB, Glazier JB, Maloney JE, et al. Effect of extra-alveolar vessels on distribution of blood flow in the dog lung. *J Appl Physiol* 1968; 25:701–712.
14. Edmunds LH, Graf PD, Nudel JA. Reinnervation of the reimplanted canine lung. *J Appl Physiol* 1971; 31:722–727.
15. Burke CM, Glanville AR, Theodore J, Robin ED. Lung immunogenicity, rejection, and obliterative bronchiolitis. *Chest* 1987; 92:3, 547–549.
16. Bergofsky EH. Thoracic deformities. In: Roussos C, Macklem PT, eds. *The thorax, Part B.* New York: Marcel Dekker, 1985:941–978.
17. McLean JR. Pulmonary vascular innervation. In: Bergofsky EH, ed. *Abnormal pulmonary circulation.* New York: Churchill Livingstone, 1986:27–81.